THE JOURNAL OF BIOLOGICAL CHEMISTRY VOL. 284, NO. 44, pp. 30177–30186, October 30, 2009

Pigment Epithelium-derived Factor Maintains Retinal Pigment Epithelium Function by Inhibiting Vascular Endothelial Growth Factor-R2 Signaling through γ-Secretase*

Received for publication, June 11, 2009, and in revised form, August 28, 2009 Published, JBC Papers in Press, September 1, 2009, DOI 10.1074/jbc.M109.032391

Zsolt Ablonczy[‡1], Annamalai Prakasam[§], James Fant[‡], Abdul Fauq[¶], Craig Crosson[‡], and Kumar Sambamurti[§]

From the Departments of [‡]Ophthalmology and [§]Neuroscience, Medical University of South Carolina, Charleston, South Carolina 29425 and the [¶]Department of Neuroscience, Mayo Clinic, Jacksonville, Florida 32224

Wet age-related macular degeneration (AMD) attacks the integrity of the retinal pigment epithelium (RPE) barrier system. The pathogenic process was hypothesized to be mediated by vascular endothelial growth factor (VEGF) and antagonized by pigment epithelium-derived factor (PEDF). To dissect these functional interactions, monolayer cultures of RPE cells were established, and changes in transepithelial resistance were evaluated after administration of PEDF, placenta growth factor (VEGF-R1 agonist), and VEGF-E (VEGF-R2 agonist). A recently described mechanism of VEGF inhibition in endothelia required the release of VEGF-R1 intracellular domain by γ-secretase. To evaluate this pathway in the RPE, cells were pretreated with inhibitors DAPT or LY411575. Processing of VEGF receptors was assessed by Western blot analysis. Administration of VEGF-E rapidly increased RPE permeability, and PEDF inhibited the VEGF-E response dose-dependently. Both γ-secretase antagonists prevented the inhibitory effects of PEDF. The co-administration of PEDF and VEGF-E depleted the amount of VEGF-R2 in the membrane and increased the amount of VEGF-R2 ectodomain in the media. Therefore, the inhibitory effect of PEDF appears to be mediated via the processing of VEGF-R2 by γ-secretase. γ-Secretase generates the amyloid-β (Aβ) peptide of Alzheimer disease from its precursor (amyloid precursor protein). This peptide is also a component of drusen in dry AMD. The results support the hypothesis that misregulation of γ-secretase may not only lead to Aβ deposits in dry AMD but can also be damaging to RPE function by blocking the protective effects of PEDF to prevent VEGF from driving the dry to wet AMD transition.

Age-related macular degeneration (AMD)[2] is often diagnosed by the appearance of subretinal fluid. This fluid causes a local detachment of the retina in the macular area resulting in decreased visual acuity in the center of the visual field (1). The resulting macular edema can lead to complete vision loss (2). Although the excessive fluid mainly comes from capillaries in the inner retina, the removal of subretinal fluid is dependent on the RPE. The maintenance of RPE barrier function is essential for the efficient removal of the fluid (3), and the disruption of the RPE barrier can eventually lead to choroidal neovascularization.

Recent clinical studies have shown that intravitreally administered anti-VEGF compounds are effective therapies for choroidal neovascularization (4–6). Originally, VEGF was described as an endothelial angiogenic and vasopermeability factor. The leakage through the vessels of the inner retina increases in response to VEGF (7, 8). However, the release of VEGF also affects RPE function (9–11). We have recently shown that RPE barrier integrity is modulated by VEGF through apically oriented VEGF-R2 receptors (12). Thus, there is a growing body of evidence that intraocular VEGF can increase the permeability of both the inner and outer blood-retina barriers, contributing to the accumulation of subretinal fluid and macular edema.

Pigment epithelium-derived factor was initially identified as a neurotrophic agent secreted by fetal human RPE cells (13). Subsequent experiments have recognized that PEDF is an endogenous antagonist of VEGF (14). In the eye, studies have provided evidence that endothelial quiescence and barrier function is achieved through a balance of VEGF and PEDF (15). The PEDF secretion pattern from the RPE cells is predominantly apical, and the interphotoreceptor matrix around the RPE microvilli is a major reservoir of PEDF (16, 17). Therefore, we hypothesize that PEDF can antagonize the breakdown of RPE function induced by the apical actions of VEGF.

Several schemes have been proposed for the anti-VEGF activity of PEDF. A PEDF receptor has been identified, which has phospholipase A_2 activity (18). PEDF binding proteins without clear receptor activity have also been found (19). In endothelial cells, PEDF has also been shown to compete with VEGF for binding at the VEGF-R2 receptor (20). PEDF was found to regulate VEGF expression (20, 21) and decrease VEGF receptor phosphorylation (14). A recent study in endothelia has elucidated a novel inhibitory mechanism of VEGF signaling via

* This work was supported, in whole or in part, by National Institutes of Health Grants EY14793, AG023055, and EY009741 from NEI, NIA, and NEI, respectively. This work was also supported by Medical University of South Carolina (MUSC) Grant URC P28918 and an unrestricted grant to MUSC from Research to Prevent Blindness, New York, NY. The Leica DM LFSA confocal microscope was obtained through a supplement to NIH/NEI EY13520.

[1] To whom correspondence should be addressed: 167 Ashley Ave., SEI 518E, Charleston, SC 29425. Tel.: 843-792-0777; Fax: 843-792-1723; E-mail: ablonczy@musc.edu.

[2] The abbreviations used are: AMD, age-related macular degeneration; VEGF, vascular endothelial growth factor; PEDF, pigment epithelium-derived factor; TER, transepithelial resistance; DAPT, (3,5-difluorophenylacetyl)-L-alanyl-L-2-phenylglycine *t*-butylester; APP, amyloid precursor protein; Aβ, amyloid-β; CTFα, C-terminal fragment after α-secretase cleavage of APP; BEL, bromoenol lactone; RPE, retinal pigment epithelium; ADAM, a disintegrin and metalloproteinase; PBS, phosphate-buffered saline; BEL, bromoenol lactone; DMSO, dimethyl sulfoxide.

the PEDF-induced intramembrane proteolysis of VEGF-R1 by γ-secretase (22). The goal of our study is to determine if PEDF acts as an anti-permeability agent in the RPE and to begin to understand the cellular mechanism involved in this response.

EXPERIMENTAL PROCEDURES

Tissue Culture—Culture conditions were similar to those published previously (12). The ARPE-19 cells (American Type Culture Collections, Manassas, VA) were cultured according to the vendor's instructions. Primary porcine RPE cultures were established from porcine eyes obtained from a local abattoir (Burbage Meats, Ravenel, SC). The primary cells were not passaged. Both ARPE-19 and primary RPE cells were plated on permeable-membrane inserts (Costar Clear Transwell, 0.4-μm pore, Thermo Fisher Scientific, Fair Lawn, NJ) or culture dishes (Corning Cellbind 60 mm, Fisher) containing Dulbecco's modified Eagle's medium/F-12/Ham (Sigma) with 1% fetal bovine serum (Amersham Biosciences), 1.2 g/liter sodium bicarbonate (Fisher), and 10 ml/liter L-glutamine-penicillin-G-streptomycin (2 mM, 100 units/ml, 0.1 mg/ml, respectively, Sigma) in a humidified incubator, kept at 37 °C in 5% CO_2. The media was changed every 2–3 days.

Barrier Function—Transepithelial resistance (TER) and inulin permeability measurements assessed barrier function. TER was monitored with an epithelial volt-ohmmeter (WPI, Sarasota, FL) equipped with an STX2 electrode (WPI). Resistance values for individual wells were determined from four independent measurements and corrected for the inherent resistance of the membrane inserts. For each condition, at least three independent experiments were performed. Values are expressed as the mean ± S.E. and compared by using Student's *t* test. A p value of <0.05 was considered statistically significant. Only confluent monolayer cultures with stable TER values (reached within 3 weeks for ARPE 19 cells and 8 weeks for primary RPE cells (12)) were used.

Cell Treatments—VEGF (human VEGF-A_{165}, Sigma), placenta growth factor (PlGF-1, Fitzgerald Industries International, Inc., Concord, MA), or VEGF-E (Fitzgerald) was administered to the apical or basal sides of membrane inserts with confluent monolayers (50 pg/ml to 50 ng/ml) in the absence or presence of PEDF (0.01–10 ng/ml, BioProducts, Middleton, MD). Baseline transepithelial resistance was measured at −60 min, and immediately prior to agonist administration ($t = 0$). Following this treatment, resistance was measured at 2 h. To evaluate the actions of the γ-secretase inhibitors, cultures were pretreated 60 min prior to the above treatments with DAPT (1 nM to 10 μM, Peptide International, Louisville, KY), LY411575 (100 pM to 1 μM), or vehicle (0.1% dimethyl sulfoxide, Sigma). To evaluate the phospholipase A_2 action of the PEDF receptor, cells were pretreated 60 min prior to the above treatments with 25 μM BEL (Sigma) or vehicle (phosphate-buffered saline (PBS)). Concentration-dependence curves were analyzed with Prism 4.02 (GraphPad Software Inc., San Diego, CA).

Carboxyl-[^{14}C]Inulin Permeability—The inulin permeability was determined from the apical to basolateral movement of inulin measured over 100 min using carboxyl-[^{14}C]inulin (50 μCi, 1.6 mCi/g, Moravek Biochemicals, Brea, CA). Aliquots of radioactive inulin, containing 0.5 μCi, were diluted with 100 times as much cold inulin (MP Biochemicals, Solon, OH) and added to the apical chambers of membrane inserts with confluent ARPE-19 cell monolayers 5 h after treatment with apical VEGF (10 ng/ml); apical VEGF (10 ng/ml) and apical PEDF (5 ng/ml); or vehicle (PBS). The 5-h delay between the VEGF and inulin administrations ensured that inulin flux was measured in steady state, because TER was previously found to change little between 5 and 24 h after VEGF administration (12). Aliquots of 100 μl were removed from the basolateral chamber at the time of inulin administration, and every 20 min afterward up to 100 min and replaced by equal amounts of media without inulin. The samples were placed into 24-well microplates (Packard, Meriden, CT), mixed with 900 μl of Microscint-20 scintillation fluid (Packard), and counted in a scintillation chamber (TopCount, Packard). Values are expressed as the mean of six, independent wells ±S.E. and compared by the Student *t* test. Inulin flux was determined from linear regression analysis of the amount of inulin present in the basolateral chamber *versus* elapsed time.

Immunohistochemistry—Porcine eyes were enucleated, and their anterior segment was removed. Thereafter, the eyecups were fixed in 2% paraformaldehyde (Mallinckrodt Baker, Phillipsburg, NJ) in PBS overnight at 4 °C. The following day they were washed three times in PBS at room temperature, and then treated with 30% sucrose (Sigma) overnight at 4 °C. The next day the eyecups were washed three times in PBS at room temperature, embedded in Tissue-Tek optimal cutting temperature compound (Sakura Finetek, Torrence, CA) and frozen, and 12-μm slices were cut horizontally in an HM550 cryostat (Microm, Walldorf, Germany). The slices were placed on microscope slides, washed three times in PBS at room temperature, and permeabilized by exposure to 0.2% Triton X-100 (VWR, West Chester, PA) in PBS for 30 min at 4 °C. Thereafter, the slices were washed in PBS (three times) at room temperature, and incubated with primary antibody (rabbit anti-VEGF-R2, diluted 1:100, Chemicon, Temecula, CA) for 1 h at 4 °C (negative controls were incubated with PBS only). The slides were then washed three times in PBS again, and incubated with secondary antibody (rhodamine-conjugated goat anti-rabbit, diluted 1:50, Chemicon) for 30 min at room temperature. The slides were treated with nuclear stain (DRAQ5, Biostatus, Shepshed, UK) and examined using a Leica SP2 confocal microscope (Leica Microsystems, Wetzlar, Germany) and software (LCS 2.6).

Immunoblots of Cell Media—Monolayers were grown to confluence on membrane inserts. The apical and basolateral media was replaced with fresh serum-free media (2 ml each), and the cells were subjected to four different treatments according to schedules described under "Cell Treatments": VEGF-E (5 ng/ml); PEDF (1 ng/ml); PEDF (1 ng/ml) and VEGF-E (5 ng/ml); DAPT (1 μM) and PEDF (1 ng/ml) and VEGF-E (5 ng/ml). At the close of the 2-h treatment, the apical and basolateral media (2 ml each) was collected into individual centrifuge tubes. To remove cell debris, the media was centrifuged for 5 min at 2800 × *g*, the supernatant was collected and concentrated down to a volume of 130 μl with 30-min centrifugation at 2800 × *g* through a 50,000 Da cut-off Amicon filter

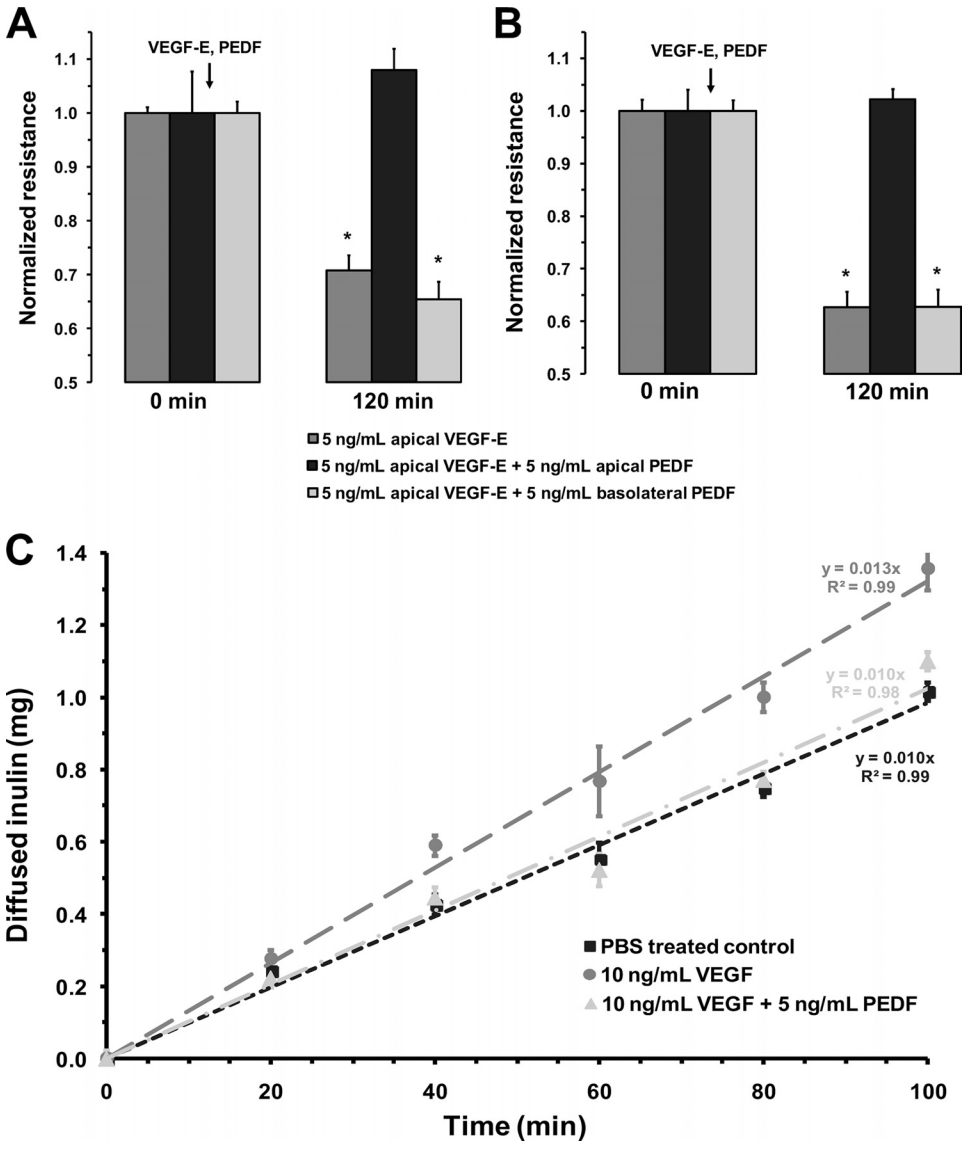

FIGURE 1. **PEDF inhibits the RPE response to VEGF-E.** The RPE response and the inhibition are polarized and VEGF-R2-dependent. Transepithelial resistance measurements on ARPE-19 (*A*) and porcine primary RPE cell monolayers (*B*) grown on permeable membrane filters. The cells were treated with apical VEGF-E (5 ng/ml) and apical or basal PEDF (5 ng/ml). The drop in resistance induced by VEGF-E was blocked by only apically administered PEDF. Values are means ± S.E. of individual measurements normalized to the average TER at $t = 0$ (*, $p < 0.01$). *C*, inulin flux through ARPE-19 cell monolayers. The apical to basolateral movement of carboxyl-[^{14}C]inulin was assessed after treatment with apical VEGF (10 ng/ml); apical VEGF (10 ng/ml) and apical PEDF (5 ng/ml); or vehicle. The inulin flux, determined from the slope of the regression analysis, was 570 μg/h for VEGF-PEDF co-treatment, which compares to the 580 μg/h measured for vehicle-treated controls. Because the inulin flux was 780 μg/h after VEGF treatment, these results mean that PEDF prevented the 36% reduction in barrier function 5 h after VEGF administration.

(Millipore, Billerica, MA). Entire volumes of concentrated media was separated on 7% Tris-acetate gels and analyzed by Western blotting using an antibody against the ectodomain of the VEGF-R2 receptor (Sigma) or VEGF-R1 receptor (Chemicon) to determine levels and fragmentation of the VEGF receptors obtained through the individual treatments. Recombinant human VEGF-R2 and VEGF-R1 (R&D Systems, Minneapolis, MN) was used as positive control. The lanes were visualized with a VersaDoc 5000 imager (Bio-Rad, Hercules, CA) after treatment with chemiluminescent reagent (Amersham Biosciences) and analyzed with the Quantity One 4.4.1 software. For each condition, at least three, independent experiments were performed. Values are expressed as the mean ± S.E. and compared by using Student's *t* test. A p value of <0.05 was considered significant.

Immunoblots of Cell Membranes—For these experiments, monolayers were grown to confluence on 100-mm culture dishes. The cells were incubated overnight with serum-free media, and then the media were replaced with fresh serum-free media, and the cells were subjected to four different treatments according to schedules described under "Cell Treatments": vehicle (0.1% DMSO); VEGF-E (5 ng/ml); DAPT (1 μM) and PEDF (1 ng/ml) and VEGF-E (5 ng/ml); PEDF (1 ng/ml) and VEGF-E (5 ng/ml). At the close of the treatment, the cultures were washed with PBS and lysed with the addition of 1 ml of buffer (2.42 g/liter Tris Base, 1 mM EGTA, 2.5 mM EDTA, 5 mM dithiothreitol, 0.3 M sucrose, 1 mM Na_3VO_4, 20 mM NaF, 1 complete mini protease inhibitor tablet, pH 7.5; the chemicals were obtained from Sigma, and the protease inhibitor was from Roche Applied Science). The cells were scraped, collected into centrifuge tubes, triturated with a 26-gauge needle syringe, and centrifuged for 5 min at 11,000 × *g*, and the supernatant was collected. Equal quantities of the various samples (determined by protein assay) were separated on 7% Tris-acetate gels and analyzed by antibodies against the C terminus of VEGF-R2 and VEGF-R1 (both from Chemicon), or the amyloid precursor protein (APP, Genway, San Diego, CA). For each condition, at least three independent experiments were performed. Values are expressed as the mean ± S.E. and compared by using Student's *t* test. A p value of <0.05 was considered statistically significant.

RESULTS

Functional Response of Polarized RPE Cells to PEDF—VEGF has been shown to induce RPE barrier failure through apical VEGF-R2 receptors (12). Thus, ARPE-19 and porcine primary RPE cells were grown on permeable membrane filters and treated with apical VEGF-E (5 ng/ml), and apical or basal PEDF (5 ng/ml). Fig. 1 shows TER measurements on ARPE-19 (Fig. 1*A*) and porcine primary RPE cell monolayers (Fig. 1*B*). In both

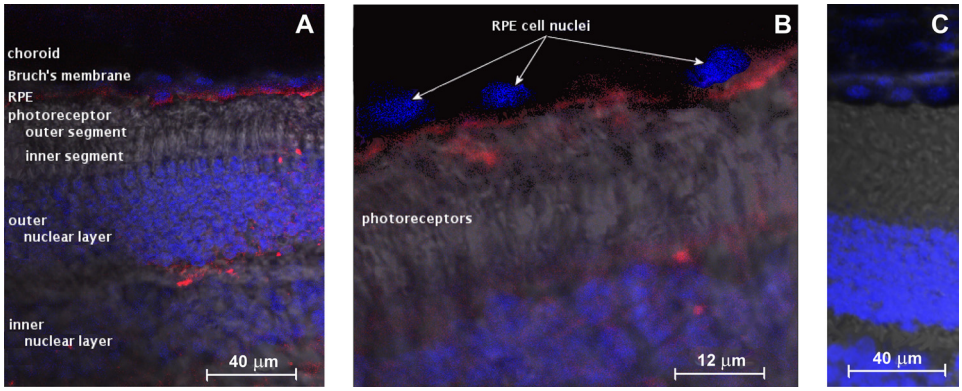

FIGURE 2. **Immunohistochemical localization of VEGF-R2 in sections of porcine eyecups.** *A–C*, images are overlays of simultaneous VEGF-R2 (*red*, rhodamine-conjugated secondary antibody), nuclear stain (*blue*), and transmitted-light microscopy photos. Only the apical surface of the RPE is stained for VEGF-R2, but VEGF-R2 staining is abundant in all layers of the neural retina, as seen in *A*. *B*, enlargement of the RPE and photoreceptors, to show VEGF-R2 localization in the RPE. *C*, negative staining control without the anti-VEGF-R2 primary antibody.

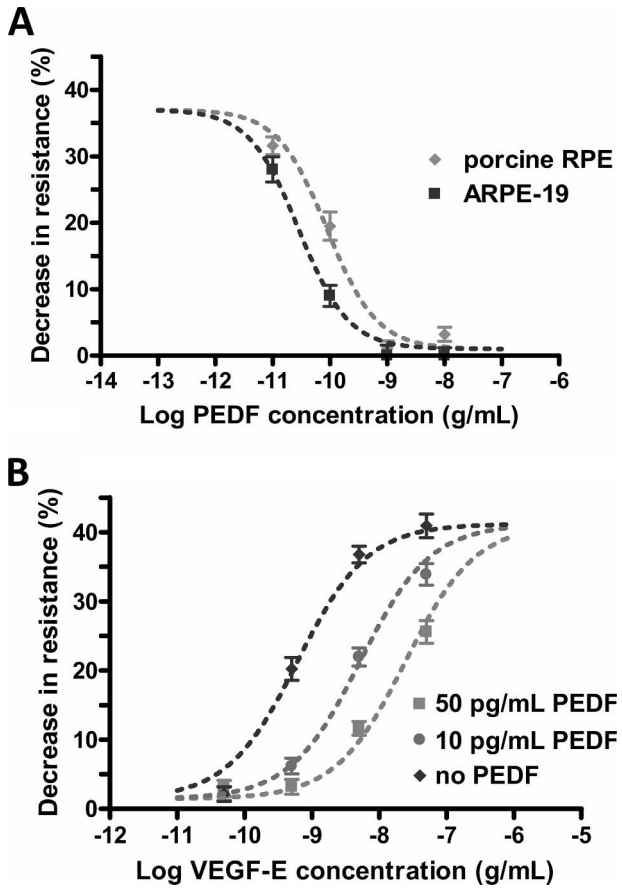

FIGURE 3. **Concentration-dependent PEDF response.** *A*, the VEGF-E-induced RPE barrier breakdown depends on the concentration of apical PEDF. ARPE-19 and primary porcine RPE cell monolayers were simultaneously treated with VEGF-E (5 ng/ml) and various concentrations of PEDF (10 pg/ml to 10 ng/ml). The figure shows the percent resistance drop at 2 h relative to the resistance before the treatments. Log IC_{50} = −10.54 ± 0.06 (29 pg/ml) for ARPE-19 cells and −10.05 ± 0.1 (89 pg/ml) for primary porcine RPE cell monolayers. The Hill coefficients were not significantly different from 1.0. *B*, Gaddum/Schild competitive model for the interaction of VEGF and PEDF in ARPE-19 cells. Monolayers were treated with various concentrations of VEGF-E (50 pg/ml to 50 ng/ml) and PEDF (0–50 pg/ml). The figure shows the percent resistance drop at 2 h relative to the resistance before the treatments. The data were analyzed with the Gaddum/Schild competitive inhibition model of the entire family of curves resulting in pA_2 = 11.85 ± 0.30 and SchildSlope = 1.03 ± 0.22. Thus, PEDF is a competitive inhibitor of VEGF-R2 with K_b = 1.4 ± 0.7 pg/ml in ARPE-19 cell monolayers. Values are the mean ± S.E. normalized to the average resistance at t = 0.

cultures, apically administered VEGF-E reduced the paracellular resistance. This TER drop was blocked by the apical administration of PEDF. Basolateral administration of PEDF did not significantly alter the VEGF-E-induced drop in TER in either culture type. No significant change in resistance was measured after apical treatment with placenta growth factor (5 ng/ml) followed by either apical or basal administration of PEDF (data not shown).

The paracellular flux of carboxyl-[^{14}C]inulin in ARPE-19 cell monolayers is a direct measure of barrier function (Fig. 1*C*). In vehicle-treated (PBS) monolayers, mean inulin flux was 580 μg/h. Administration of apical VEGF (10 ng/ml) produced a 36% increase in inulin flux to 780 μg/h. On the other hand, co-treatment of the monolayers with both apical VEGF (10 ng/ml) and apical PEDF (5 ng/ml) resulted in a flux of 570 μg/h, which was similar to the inulin flux in the vehicle-treated controls.

The results that only apical treatment with PEDF could antagonize the apical VEGF-R2-dependent RPE cell response (Fig. 1) and that PEDF could compete with VEGF for binding at the VEGF-R2 receptor (20), favors a mechanism in which the polarity of the VEGF and PEDF response is determined by VEGF-R2 localization. Cross-sections of porcine eyecups (Fig. 2) were used to investigate the localization of VEGF-R2 *in vivo*. The transmitted light layer of the image revealed the non-pigmented photoreceptor inner and outer segments, and the pigmented RPE/choroid. In the RPE, only the apical surface was stained *red* indicating the presence of VEGF-R2 in relation to the cell nuclei (*blue* stain). In control eyecups, processed without the VEGF-R2 primary antibody, no staining was observed in the RPE, although the blue cell nuclei were visible at the same exciting light intensity.

PEDF Inhibits the VEGF-R2-dependent Reduction in TER—In a cell-free system, PEDF at concentrations between 10^{-8} and 10^{-6} M competed with VEGF for binding at VEGF-R2 (20). ARPE-19 and primary porcine RPE cell monolayers were treated with VEGF-E (5 ng/ml) and various concentrations of PEDF (0.01–10 ng/ml). To assess functional responses, Fig. 3*A* shows the percent change in TER at 2 h relative to pretreatment control values. In both culture systems, the TER decrease induced by VEGF-E was dose-dependently inhibited by PEDF. Log IC_{50} was −10.54 ± 0.06 (IC_{50} = 29 pg/ml, 0.6 pM) for ARPE-19 cells and −10.05 ± 0.1 (IC_{50} = 89 pg/ml, 1.9 pM) for porcine primary RPE cells. The Hill coefficients of the concentration-response curves were not significantly different from 1.

This interaction was further studied by determining the VEGF-E concentration-induced responses in ARPE-19 cells under control conditions, and in the presence of two different concentrations of PEDF (10 and 50 pg/ml). Fig. 3*B* shows the drop in percent reduction in TER at 2 h in the presence and absence of PEDF. Gaddum-Schild analysis of these responses

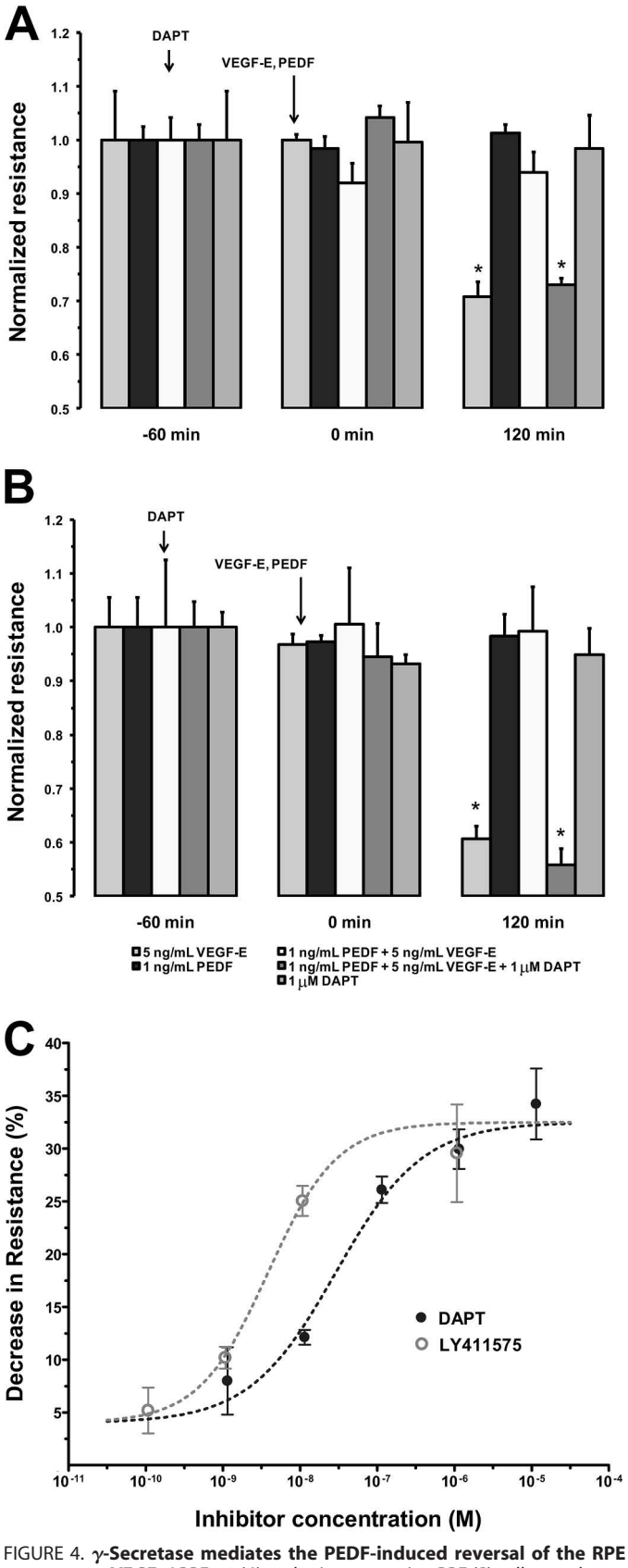

FIGURE 4. **γ-Secretase mediates the PEDF-induced reversal of the RPE response to VEGF.** ARPE-19 (*A*) and primary porcine RPE (*B*) cell monolayers were pretreated with DAPT (1 μM) or vehicle (0.1% DMSO) 1 h prior to simultaneous PEDF (1 ng/ml) and VEGF-E (5 ng/ml) treatments. VEGF-E (5 ng/ml), PEDF (1 ng/ml), and DAPT (1 μM) were used as controls. The γ-secretase inhibitor, DAPT, prevented PEDF from blocking the VEGF-E-induced TER drop. The controls did not significantly change the resistance. Values are the mean ± S.E. of individual measurements normalized to the TER at $t = -60$ min (*, $p < 0.01$). *C*, the reversal of the effect of PEDF is concentration-dependent. γ-Secretase antagonists, DAPT and LY411575, were utilized in various concentrations (100 pM to 10 μM) to reverse the inhibitory effects of PEDF on RPE barrier breakdown. The figure shows the percent resistance drop at 2 h relative to the resistance before the treatments. Log EC_{50} was -8.41 ± 0.12 ($EC_{50} = 4$ nM) for LY411575 and -7.54 ± 0.12 ($IC_{50} = 29$ nM) for DAPT, as LY411575 is a more potent inhibitor than DAPT. The Hill coefficients calculated from the concentration response curves were 0.97 for LY411575 and 0.78 for DAPT.

revealed a pA_2 value (the negative logarithm of the concentration of an antagonist required to cause a two-fold rightward shift of the agonist dose-response curve) of 11.85 ± 0.30 and a slope 1.03 ± 0.22 of for PEDF. Thus, the pharmacologic responses to PEDF are consistent with a competitive inhibitor and the calculated binding affinity was $K_b = 1.4 \pm 0.7$ pg/ml. The concentration-response data showed that 1 ng/ml PEDF induced a maximal inhibition of the VEGF-induced TER decrease. Therefore, in subsequent mechanistic experiments, we used 1 ng/ml concentration of PEDF.

γ-Secretase Inhibitors Reverse the Effect of PEDF on RPE Barrier Function—The Gaddum-Schild analysis revealed that the actions of PEDF are consistent with a competitive VEGF-R2 antagonist. However, the VEGF response was reversed by PEDF at concentrations 100–1000 times lower than required to inhibit VEGF binding to VEGF-R2. Recent studies in endothelial cells have provided evidence that PEDF induces shedding of VEGF-R1 via the activation of γ-secretase (22). Because shed receptors may act as competitive blockers sequestering VEGF, we evaluated whether γ-secretase activation was needed for PEDF to suppress VEGF actions in RPE cells.

Monolayers of ARPE-19 (Fig. 4*A*) and primary porcine (Fig. 4*B*) RPE cells were pretreated with the γ-secretase inhibitor DAPT (1 μM) or vehicle (0.1% DMSO) 1 h prior to treatment with PEDF (1 ng/ml) and/or VEGF-E (5 ng/ml). Pretreatment with DAPT prevented PEDF from blocking the VEGF-E-induced reduction in TER. Neither PEDF nor DAPT alone could significantly alter the resistance readout. To confirm these results, monolayer cultures of ARPE-19 cells were pretreated with various concentrations of DAPT or LY411575 1 h prior to treatment with PEDF (1 ng/ml) and VEGF-E (5 ng/ml). LY411575 is a γ-secretase inhibitor more potent than DAPT (23). As shown in Fig. 4*C* both antagonists reversed the inhibitory action of PEDF on the VEGF-induced barrier breakdown in a concentration-dependent manner. However, the response for LY411575 ($EC_{50} = 4$ nM) was left shifted when compared with DAPT ($EC_{50} = 29$ nM).

Protease Activity in Response to Treatment with PEDF and VEGF-E—The activity of γ-secretase was quantitated by measuring APP processing (24). APP is cleaved by α-secretase to produce the soluble sAPPα and the membrane-bound C-terminal fragment (CTFα), which is further processed by γ-secretase. Thus, the activity of γ-secretase is inversely proportional to the amount of CTFα. Confluent ARPE-19 cell monolayers were pretreated with DAPT (1 μM) or vehicle (0.1% DMSO) 60 min prior to treatment with VEGF-E (5 ng/ml) and/or PEDF (1 ng/ml). Fig. 5 (*A* and *B*) shows that the addition of VEGF-E alone produced a small but not significant increase in γ-secretase activity. Co-administration of PEDF and VEGF-E for 2 h

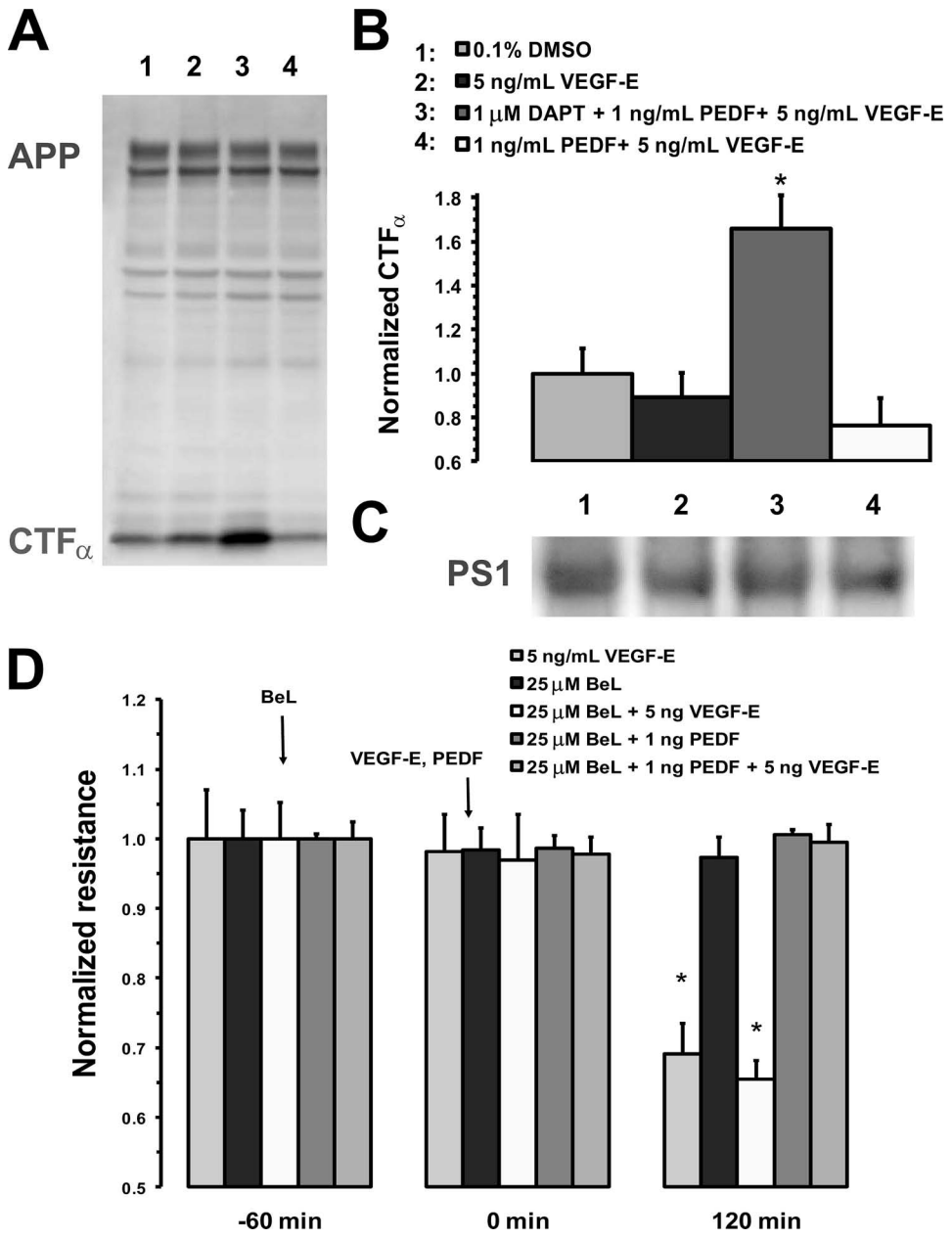

FIGURE 5. **Co-administration of VEGF and PEDF induces γ-secretase activity.** *A*, γ-secretase activity was probed with a C-terminal APP antibody against the membrane fraction from confluent ARPE-19 cell monolayers. The cells were pretreated with DAPT (1 μM) or vehicle (0.1% DMSO) 1 h prior to PEDF (1 ng/ml) or VEGF-E (5 ng/ml) treatment for 2 h. The *lanes* represent individual cultures treated by *1*, 0.1% DMSO (vehicle); *2*, VEGF-E (5 ng/ml); *3*, PEDF (1 ng/ml) and VEGF-E (5 ng/ml) and DAPT (1 μM); and *4*, PEDF (1 ng/ml) and VEGF-E (5 ng/ml). The gel micrograph shows bands for the full-length APP protein (78 kDa), and the CTFα fragment (11 kDa). *B*, summary of the γ-secretase activity data. Six independent experiments were performed similar to *panel A*, and the densities for the APP and CTFα bands were analyzed. The activity of γ-secretase is inversely proportional to the amount of CTFα present. DAPT antagonized γ-secretase activity (*lane 3*). The PEDF and VEGF-E treatments alone did not significantly change γ-secretase activity from vehicle-treated controls, however, PEDF and VEGF-E together induced a 24% increase in γ-secretase activity. Values are the mean ± S.E. of individual measurements (*, $p < 0.05$ compared with VEGF treatment). *C*, the expression of presenilin-1 (*PS1*) did not significantly change in response to the above treatments. The *gel micrograph* shows the bands for full-length presenilin-1 (46 kDa). *D*, the effects of PEDF are not mediated by the catalytic activity of the PEDF receptor. ARPE-19 cell monolayers were pretreated with 25 μM bromoenol lactone (BEL) 1 h prior to PEDF (1 ng/ml), VEGF-E (5 ng/ml), or simultaneous PEDF (1 ng/ml) and VEGF-E (5 ng/ml) treatments. BEL is an inhibitor of the catalytic phospholipase A_2 activity of the PEDF receptor in the RPE. The responses to VEGF and/or PEDF are not significantly different from cultures that were not pretreated with BEL. Values are the mean ± S.E. of individual measurements normalized to the TER at $t = -60$ min (*, $p < 0.01$).

increased γ-secretase activity by 24%, in agreement with the results of Cai *et al.* (22) extrapolated for this short time period. Pretreatment with DAPT blocked γ-secretase activity and caused an accumulation of CTFα, as expected. Similar to Cai *et al.* (22), PEDF did not significantly change γ-secretase activity in 2 h (data not shown). Fig. 5*C* confirms that the expression of the catalytic subunit of γ-secretase, presenilin-1, did not significantly change during the incubation period.

To assess whether the activation of a recently reported PEDF receptor (18) is required to antagonize RPE barrier failure, monolayer cultures of ARPE-19 cells were pretreated with BEL, a phospholipase A_2 inhibitor. Phospholipase A_2 activity has been a measure of receptor stimulation (18). Fig. 5*D* indicates that 1-h pretreatment with BEL (25 μM) prior to treatment with PEDF (1 ng/ml) and/or VEGF-E (5 ng/ml) did not significantly alter the ability of PEDF to inhibit the TER decrease induced by VEGF-E.

PEDF and VEGF-E Induce VEGF-R2 Shedding—Reported γ-secretase substrates are generally first processed close to the cell surface to shed their ectodomain. Then, the membrane-bound C-terminal fragment is processed by γ-secretase to release the intracellular domain (25).

Our physiological data provided evidence that, in RPE cells, VEGF-R2 can be a target of γ-secretase. To begin to understand this process, we studied the release of VEGF-R2 ectodomain into the media of the membrane inserts in response to 2-h treatments with PEDF (1 ng/ml) and VEGF-E (5 ng/ml) and 1-h pretreatment with DAPT (1 μM) or vehicle (0.1% DMSO). Fig. 6*A* shows representative Western blot bands obtained with an antibody against the ectodomain of VEGF-R2 in the apical media. A broad band at 160 kDa is shown consistently with a previous report for soluble VEGF-R2 (26). Fig. 6*B* presents the quantitation of data obtained in three independent experiments normalized to the levels found in the VEGF-E-treated controls. The amount of VEGF-R2 ectodomain was not significantly different after vehicle treatment (data not shown). Co-treatment with PEDF and VEGF-E led to an

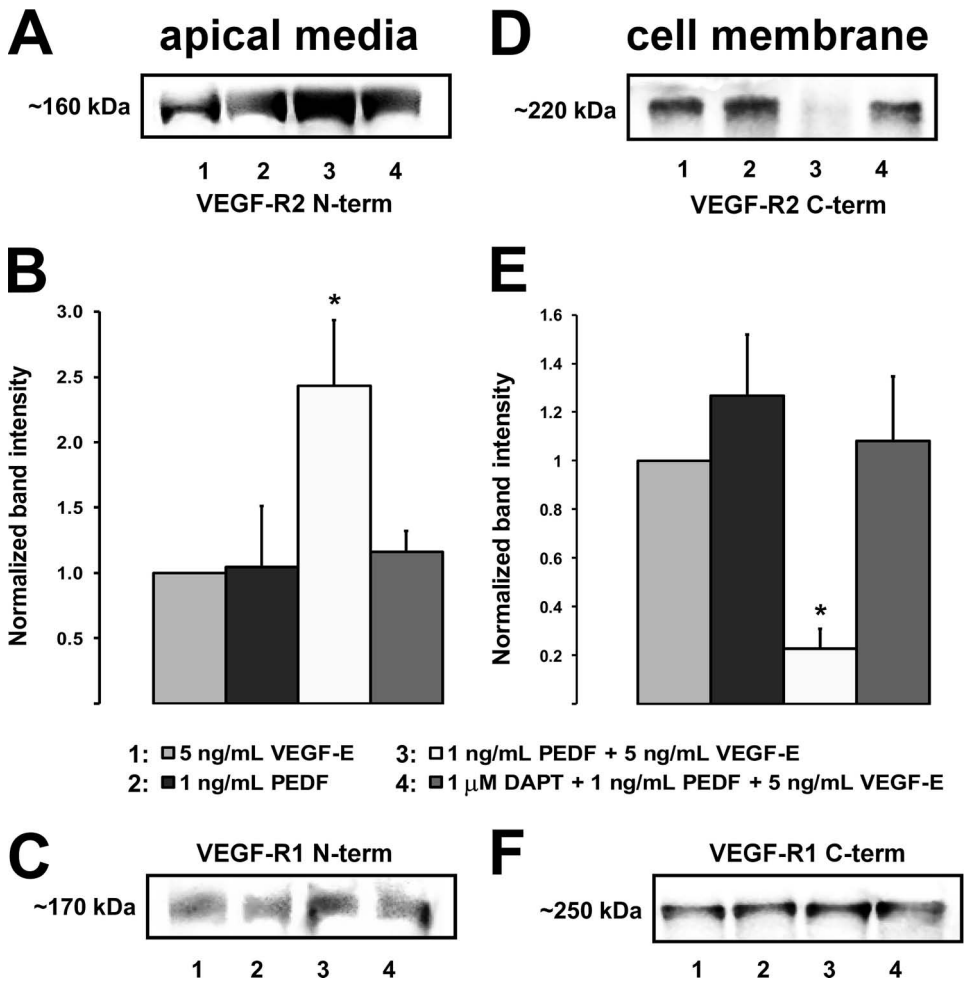

FIGURE 6. **VEGF-R2 receptor shedding after co-administration of VEGF and PEDF.** VEGF-R2 ectodomain appears in the apical media of RPE cells after simultaneous PEDF and VEGF-E treatments. *A*, Western blot of apical media from ARPE-19 cell monolayers pretreated with DAPT (1 μM) or vehicle (0.1% DMSO) 1 h prior to PEDF (1 ng/ml) or VEGF-E (5 ng/ml) treatments for 2 h and probed with an N-terminal VEGF-R2 antibody. One band was observed at 160 kDa. The *lanes* represent individual cultures and were treated by *1*, VEGF-E (5 ng/ml); *2*, PEDF (1 ng/ml); *3*, PEDF (1 ng/ml) and VEGF-E (5 ng/ml) and DAPT (1 μM); and *4*, PEDF (1 ng/ml) and VEGF-E (5 ng/ml). *B*, summary of the VEGF-R2 immunoblots. Three independent experiments were performed similar to *panel A*, and the density for the band (at 160 kDa) was analyzed. PEDF and VEGF-E together induced an increase in VEGF-R2 bands in the media *versus* the VEGF-E treatment. Pretreatment with DAPT reversed the combined effect of PEDF and VEGF. The values are the mean ± S.E. of individual measurements (*, $p < 0.05$ compared with control). *C*, Western blot of apical media from ARPE-19 cell monolayers with an N-terminal VEGF-R1 antibody. One band was observed at 170 kDa. The *lanes* represent individual cultures and were treated similar to *panel A*. There was no significant difference between the four treatments, demonstrating that the ectodomain of the VEGF-R1 receptor is not processed after VEGF-E and PEDF treatments. On the other hand, VEGF-R2 is also processed in the cell membranes. *D*, the cell membranes of ARPE-19 cells (treated similar to *panel A*) were collected and probed with a C-terminal VEGF-R2 antibody. One band was observed at 220 kDa for the full-length receptor. *E*, summary of VEGF-R2 immunoblots from the cell membranes. Three independent experiments were performed similarly to *panel A*, and the density for the band at 220 kDa was analyzed. PEDF and VEGF-E together induced a significant decrease in the VEGF-R2 band. Pretreatment with DAPT reversed the combined effect of PEDF and VEGF. The values are the mean ± S.E. of individual measurements (*, $p < 0.05$ compared with control). *F*, Western blot of ARPE-19 cell membranes probed with a C-terminal VEGF-R1 antibody. One band was observed at 250 kDa for the full-length receptor. VEGF-R1 was unaffected by the treatments, demonstrating that it did not mediate the combined effects of VEGF and PEDF.

increase in the levels of VEGF-R2 ectodomain. This increase was blocked by 1-h pretreatment with DAPT. The basolateral media did not contain VEGF-R2 ectodomain (data not shown).

To confirm that VEGF-R2 is released from RPE membranes we examined the levels of VEGF-R2 in cellular membrane extracts using a C-terminal VEGF-R2 antibody. ARPE-19 cells were treated with PEDF (1 ng/ml) and VEGF-E (5 ng/ml) similar to the above experiments (Fig. 6*A*). Fig. 6*D* shows representative Western blot bands, and Fig. 6*E* quantitates the obtained data. Full-length VEGF-R2 at 220 kDa was observed in all lanes. VEGF or PEDF treatment alone did not change the expression of VEGF-R2 in the membrane. However, in samples co-treated with PEDF and VEGF-E, the band was significantly depleted. 1-h pretreatment with DAPT (1 μM) prevented the decrease in full-length VEGF-R2.

Although changes in TER were not observed with the VEGF-R1 agonist placenta growth factor, VEGF receptors can form heterodimers between VEGF-R1 and VEGF-R2 (27). Therefore, the possibility existed that VEGF-R1 receptor is processed after VEGF-E binding to VEGF-R2. To investigate this, VEGF-R1 ectodomain levels were determined in the apical media following treatment with VEGF-E, PEDF, and DAPT (concentrations same as above). A 170-kDa band corresponding to the ectodomain of VEGF-R1 was present in all the samples. However, the level of the band did not change in response to co-treatment with PEDF and VEGF-E or when pretreated with DAPT (Fig. 6*C*). Moreover, no release of VEGF-R1 from the membranes was observed with antibody against the VEGF-R1 C terminus. The full-length VEGF-R1 (250 kDa band) was not affected by the various treatments (Fig. 6*F*). Therefore, it appears that VEGF-R2 and not VEGF-R1 is the target of γ-secretase-mediated proteolytic processing in the RPE.

DISCUSSION

Previous *in vitro* and *in vivo* experiments have shown that in normal conditions VEGF secretion from RPE cells occurs predominantly at the basolateral side (16, 28) and is required for choriocapillaris development (28, 29). However, the secretion of PEDF from the RPE is primarily apical (16, 17). Therefore, PEDF was originally thought to be a neurotrophic factor in the retina. Subsequent studies demonstrated that PEDF is an anti-VEGF agent in the retinal vasculature (14). More recent experiments have provided evidence that VEGF secretion across the apical RPE membrane can occur under oxidative stress (30, 31). These data along with our results (VEGF

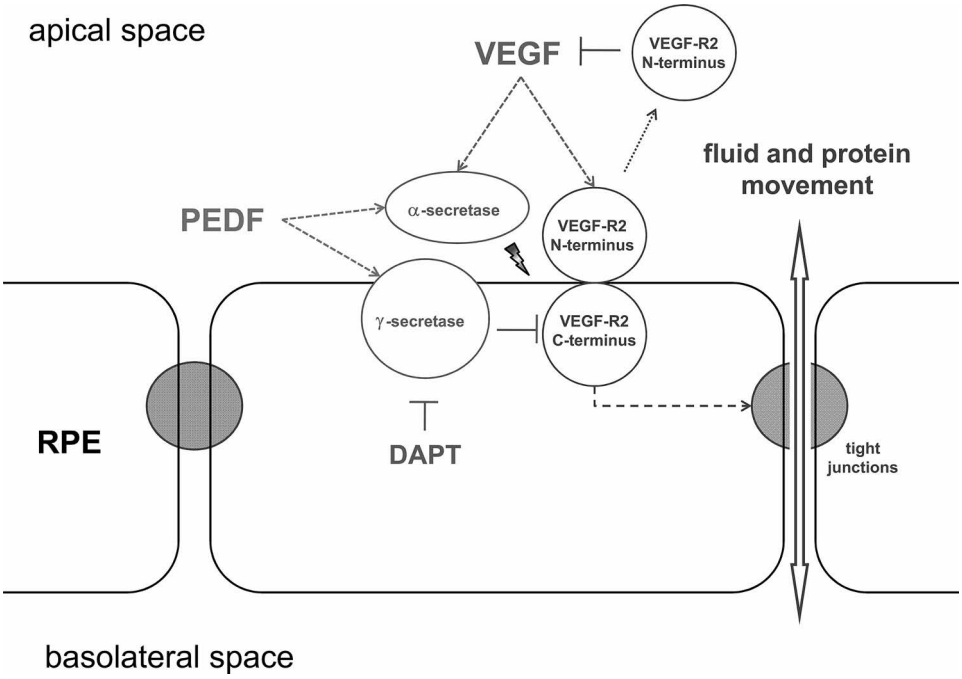

FIGURE 7. **The proposed mechanism of VEGF-R2 processing**. The combined action of PEDF and VEGF activates a yet unknown α-secretase and the known γ-secretase to shed the VEGF-R2 ectodomain and to rapidly clear the receptor from the RPE cell membrane, which eliminates the VEGF-R2-induced permeability increase. The binding of VEGF-E to the released VEGF-R2 ectodomain is responsible for the high affinity competitive inhibition. DAPT blocks γ-secretase; therefore, VEGF-R2 receptor signaling is maintained against the combined actions of PEDF and VEGF. Moreover, the γ-secretase inhibition has a negative feedback on the ectodomain shedding.

receptors are restricted to the apical surface and their activation leads to RPE barrier breakdown; apical VEGF is released in H_2O_2 treatment of RPE monolayers) (12, 32), led to the hypothesis that PEDF can play an essential autocrine role in maintaining RPE barrier function during oxidative stress.

The results of the current study demonstrate that PEDF is highly effective in preventing the VEGF-induced increases in RPE permeability in both ARPE-19 and primary porcine RPE cell monolayers (Figs. 1 and 2). The analysis of the concentration-response curves revealed that RPE cells are 10- to 100-times more sensitive to PEDF (K_b = 1.4 ± 0.7 pg/ml, or IC_{50} = 29 pg/ml) than to VEGF (EC_{50} = 502 pg/ml (12)), agreeing with the idea that PEDF can efficiently defend the RPE against VEGF-induced loss of function. Moreover, the Schild analysis of these functional data revealed that the actions of PEDF are consistent with those of a competitive inhibitor of VEGF-R2 (Fig. 3). However, the K_b obtained from our studies is two to three orders of magnitude lower than the concentration of PEDF required for the inhibition of VEGF binding to the VEGF-R2 receptor (20). This substantial enhancement in the potency of PEDF in our studies indicates that PEDF antagonized the VEGF responses by a mechanism other than direct competition for the VEGF-R2 receptor. Fig. 4 shows that γ-secretase is required for the inhibitory action of PEDF.

γ-Secretase was initially recognized, because the mutations of its presenilin subunit cause Alzheimer disease (33). The protein is responsible for the final step in processing APP into Aβ (34), aggregated forms of which accumulate in Alzheimer disease. Functionally, γ-secretase is an endopeptidase, which can digest the membrane-spanning region of any type-1 integral membrane protein, after the ectodomain has been removed (35, 36). Thus, γ-secretase is seen as the "proteasome" of cell membranes (37, 38). It is known to process a series of membrane receptors into signaling molecules that can thereafter translocate (35). In the RPE, it was known to take part in the trafficking and processing of tyrosinase enzymes, responsible for normal pigmentation (39). The data presented in our report provide evidence for the first time that PEDF inhibits VEGF-induced barrier breakdown of RPE cell monolayers through the activation of γ-secretase. In endothelial cells, the direct target of γ-secretase was VEGF-R1 (22). In the RPE cells, however, the proteolysis of VEGF-R1 was not required (Fig. 6, *C* and *F*). Although our results support the idea that an activated form of VEGF-R2 is the direct target of γ-secretase in the RPE, it cannot entirely be excluded at this time that γ-secretase action is mediated by the cleavage of a third, yet unknown protein or receptor, the activity of which is regulated by PEDF. But, our experiments provided convincing evidence that both VEGF-E and PEDF are required to expose sites on VEGF-R2 where secretases (which have a high constitutive activity (Fig. 5)) can cleave the receptor. Details of the proposed mechanism of how γ-secretase is involved with the regulation of VEGF-R2 signaling are shown in Fig. 7.

In light of the involvement of γ-secretase, it is quite surprising that the dose-response calculations show PEDF as a competitive inhibitor of the VEGF-R2-dependent TER decrease. But this apparent paradox can be explained, because γ-secretase cleavage requires the primary action of an α-secretase. α-Secretases (such as ADAM10) have been identified in other epithelial tissues (40), and matrix metalloproteinases (which are collectively referred to as ADAMs) are known to be expressed by RPE cells (41). But the expression of ADAMs, their targets, and the regulation of their activities in the RPE have not been described. In a recent report, ADAM17 has been shown to be the enzyme responsible for the VEGF-induced shedding of VEGF-R2 ectodomain in COS-7 cells (42). Our data of increased VEGF-R2 ectodomain in the apical media when both VEGF-E and PEDF were present (Fig. 6) can be attributed to a yet unknown protease. But the released ectodomain of VEGF-R2 can bind VEGF-R2 agonists, acting as an effective competitive inhibitor. In fact, the VEGF-R2 ectodomain (soluble

VEGF-R2) has been used with similar reasoning to inhibit tumor angiogenesis *in vivo* (43). Moreover, soluble VEGF-R2 has been identified in media of endothelial cells as well as from the plasma (26). Our data show that the soluble VEGF-R2, hypothesized to be a significant angiogenesis regulator, can be a result of PEDF-induced proteolysis of VEGF-R2.

The involvement of γ-secretase in the maintenance of RPE barrier function is an interesting development, because Aβ (the best known product of γ-secretase) is a component of drusen deposited in dry AMD (44–46). Our results show that if PEDF and VEGF are both present, the processing of APP CTFα is slightly accelerated; supporting the idea that PEDF- and VEGF-induced γ-secretase action may contribute to the buildup of drusen over a long time period. This implies that similar mechanisms may be responsible for plaque formation in Alzheimer disease and drusen formation in dry AMD. These results are consistent with the hypothesis that Aβ is associated with the pathogenesis of AMD (47).

In conclusion, our physiological, histochemical, and biochemical data have provided new evidence that PEDF can maintain RPE barrier function in the presence of activated VEGF-R2 receptors. The functional response of RPE cells to PEDF is polarized to the apical side, where the VEGF-R2 receptors are located, and is mediated by γ-secretase. Thus, in conditions where apical VEGF is present, PEDF allows normal RPE barrier function through inducing the proteolysis of VEGF-R2 and other membrane proteins (such as APP), contributing to the symptoms of dry AMD. Moreover, it seems that the transition from dry to wet AMD occurs when the PEDF-stimulated proteolysis of VEGF-R2 by γ-secretase is reduced, allowing unregulated VEGF signaling in the RPE. Work is ongoing in our laboratories to understand the details of the biochemical mechanism of VEGF-R2 processing by the PEDF-γ-secretase system.

Acknowledgments—We want to thank Kioina Meyers and Chitra Venugopal for technical help.

REFERENCES

1. Tranos, P. G., Wickremasinghe, S. S., Stangos, N. T., Topouzis, F., Tsinopoulos, I., and Pavesio, C. E. (2004) *Surv. Ophthalmol.* **49,** 470–490
2. Augustin, A. J., Puls, S., and Offermann, I. (2007) *Retina* **27,** 133–140
3. Marmor, M. F. (1999) *Documenta Ophthalmologica* **97,** 239–249
4. Gragoudas, E. S., Adamis, A. P., Cunningham, E. T., Jr., Feinsod, M., and Guyer, D. R. (2004) *N. Engl. J. Med.* **351,** 2805–2816
5. Heier, J. S., Antoszyk, A. N., Pavan, P. R., Leff, S. R., Rosenfeld, P. J., Ciulla, T. A., Dreyer, R. F., Gentile, R. C., Sy, J. P., Hantsbarger, G., and Shams, N. (2006) *Ophthalmology* **113,** 642, e641–644
6. Spaide, R. F., Laud, K., Fine, H. F., Klancnik, J. M., Jr., Meyerle, C. B., Yannuzzi, L. A., Sorenson, J., Slakter, J., Fisher, Y. L., and Cooney, M. J. (2006) *Retina* **26,** 383–390
7. Antcliff, R. J., and Marshall, J. (1999) *Semin. Ophthalmol.* **14,** 223–232
8. Gillies, M. C. (1999) *Documenta Ophthalmologica* **97,** 251–260
9. Ghassemifar, R., Lai, C. M., and Rakoczy, P. E. (2006) *Cell Tissue Res.* **323,** 117–125
10. Hartnett, M. E., Lappas, A., Darland, D., McColm, J. R., Lovejoy, S., and D'Amore, P. A. (2003) *Exp. Eye Res.* **77,** 593–599
11. Miyamoto, N., de Kozak, Y., Jeanny, J. C., Glotin, A., Mascarelli, F., Massin, P., BenEzra, D., and Behar-Cohen, F. (2007) *Diabetologia* **50,** 461–470
12. Ablonczy, Z., and Crosson, C. E. (2007) *Exp. Eye Res.* **85,** 762–771
13. Tombran-Tink, J., Chader, G. G., and Johnson, L. V. (1991) *Exp. Eye Res.* **53,** 411–414
14. Tombran-Tink, J. (2005) *Front. Biosci.* **10,** 2131–2149
15. Ohno-Matsui, K., Morita, I., Tombran-Tink, J., Mrazek, D., Onodera, M., Uetama, T., Hayano, M., Murota, S. I., and Mochizuki, M. (2001) *J. Cell. Physiol.* **189,** 323–333
16. Maminishkis, A., Chen, S., Jalickee, S., Banzon, T., Shi, G., Wang, F. E., Ehalt, T., Hammer, J. A., and Miller, S. S. (2006) *Invest. Ophthalmol. Vis. Sci.* **47,** 3612–3624
17. Tombran-Tink, J., Shivaram, S. M., Chader, G. J., Johnson, L. V., and Bok, D. (1995) *J. Neurosci.* **15,** 4992–5003
18. Notari, L., Baladron, V., Aroca-Aguilar, J. D., Balko, N., Heredia, R., Meyer, C., Notario, P. M., Saravanamuthu, S., Nueda, M. L., Sanchez-Sanchez, F., Escribano, J., Laborda, J., and Becerra, S. P. (2006) *J. Biol. Chem.* **281,** 38022–38037
19. Alberdi, E., Aymerich, M. S., and Becerra, S. P. (1999) *J. Biol. Chem.* **274,** 31605–31612
20. Zhang, S. X., Wang, J. J., Gao, G., Parke, K., and Ma, J. X. (2006) *J. Mol. Endocrinol.* **37,** 1–12
21. Yamagishi, S., Matsui, T., Nakamura, K., Yoshida, T., Shimizu, K., Takegami, Y., Shimizu, T., Inoue, H., and Imaizumi, T. (2006) *Microvasc. Res.* **71,** 222–226
22. Cai, J., Jiang, W. G., Grant, M. B., and Boulton, M. (2006) *J. Biol. Chem.* **281,** 3604–3613
23. Weihofen, A., Lemberg, M. K., Friedmann, E., Rueeger, H., Schmitz, A., Paganetti, P., Rovelli, G., and Martoglio, B. (2003) *J. Biol. Chem.* **278,** 16528–16533
24. Zhou, Y., Suram, A., Venugopal, C., Prakasam, A., Lin, S., Su, Y., Li, B., Paul, S. M., and Sambamurti, K. (2008) *FASEB J.* **22,** 47–54
25. Pinnix, I., Musunuru, U., Tun, H., Sridharan, A., Golde, T., Eckman, C., Ziani-Cherif, C., Onstead, L., and Sambamurti, K. (2001) *J. Biol. Chem.* **276,** 481–487
26. Ebos, J. M., Bocci, G., Man, S., Thorpe, P. E., Hicklin, D. J., Zhou, D., Jia, X., and Kerbel, R. S. (2004) *Mol. Cancer Res.* **2,** 315–326
27. Autiero, M., Waltenberger, J., Communi, D., Kranz, A., Moons, L., Lambrechts, D., Kroll, J., Plaisance, S., De Mol, M., Bono, F., Kliche, S., Fellbrich, G., Ballmer-Hofer, K., Maglione, D., Mayr-Beyrle, U., Dewerchin, M., Dombrowski, S., Stanimirovic, D., Van Hummelen, P., Dehio, C., Hicklin, D. J., Persico, G., Herbert, J. M., Communi, D., Shibuya, M., Collen, D., Conway, E. M., and Carmeliet, P. (2003) *Nat. Med.* **9,** 936–943
28. Blaauwgeers, H. G., Holtkamp, G. M., Rutten, H., Witmer, A. N., Koolwijk, P., Partanen, T. A., Alitalo, K., Kroon, M. E., Kijlstra, A., van Hinsbergh, V. W., and Schlingemann, R. O. (1999) *Am. J. Pathol.* **155,** 421–428
29. Marneros, A. G., Fan, J., Yokoyama, Y., Gerber, H. P., Ferrara, N., Crouch, R. K., and Olsen, B. R. (2005) *Am. J. Pathol.* **167,** 1451–1459
30. Kannan, R., Zhang, N., Sreekumar, P. G., Spee, C. K., Rodriguez, A., Barron, E., and Hinton, D. R. (2006) *Mol. Vis.* **12,** 1649–1659
31. Slomiany, M. G., and Rosenzweig, S. A. (2004) *Invest. Ophthalmol. Vis. Sci.* **45,** 2838–2847
32. Thurman, J. M., Renner, B., Kunchithapautham, K., Ferreira, V. P., Pangburn, M. K., Ablonczy, Z., Tomlinson, S., Holers, V. M., and Rohrer, B. (2009) *J. Biol. Chem.* **284,** 16939–16947
33. Sherrington, R., Rogaev, E. I., Liang, Y., Rogaeva, E. A., Levesque, G., Ikeda, M., Chi, H., Lin, C., Li, G., Holman, K., *et al*. (1995) *Nature* **375,** 754–760
34. De Strooper, B., and Woodgett, J. (2003) *Nature* **423,** 392–393
35. Kopan, R., and Ilagan, M. X. (2004) *Nat. Rev.* **5,** 499–504
36. Sambamurti, K., Suram, A., Venugopal, C., Prakasam, A., Zhou, Y., Lahiri, D. K., and Greig, N. H. (2006) *Curr. Alzheimer. Res.* **3,** 81–90
37. Sambamurti, K., Greig, N. H., and Lahiri, D. K. (2002) *Neuromol. Med.* **1,** 1–31
38. Small, D. H. (2002) *Peptides* **23,** 1317–1321
39. Wang, R., Tang, P., Wang, P., Boissy, R. E., and Zheng, H. (2006) *Proc. Natl. Acad. Sci. U.S.A.* **103,** 353–358
40. Dijkstra, A., Postma, D. S., Noordhoek, J. A., Lodewijk, M. E., Kauffman, H. F., ten Hacken, N. H., and Timens, W. (2009) *Virchows Arch.* **454,** 441–449

41. Ahir, A., Guo, L., Hussain, A. A., and Marshall, J. (2002) *Invest. Ophthalmol. Vis. Sci.* **43,** 458–465
42. Swendeman, S., Mendelson, K., Weskamp, G., Horiuchi, K., Deutsch, U., Scherle, P., Hooper, A., Rafii, S., and Blobel, C. P. (2008) *Circ. Res.* **103,** 916–918
43. Kou, B., Li, Y., Zhang, L., Zhu, G., Wang, X., Li, Y., Xia, J., and Shi, Y. (2004) *Exp. Mol. Pathol.* **76,** 129–137
44. Anderson, D. H., Talaga, K. C., Rivest, A. J., Barron, E., Hageman, G. S., and Johnson, L. V. (2004) *Exp. Eye Res.* **78,** 243–256
45. Dentchev, T., Milam, A. H., Lee, V. M., Trojanowski, J. Q., and Dunaief, J. L. (2003) *Mol. Vis.* **9,** 184–190
46. Johnson, L. V., Leitner, W. P., Rivest, A. J., Staples, M. K., Radeke, M. J., and Anderson, D. H. (2002) *Proc. Natl. Acad. Sci. U.S.A.* **99,** 11830–11835
47. Yoshida, T., Ohno-Matsui, K., Ichinose, S., Sato, T., Iwata, N., Saido, T. C., Hisatomi, T., Mochizuki, M., and Morita, I. (2005) *J. Clin. Invest.* **115,** 2793–2800